Pouring Height Effects on Macro-Segregation and Electrical/Thermal Properties of Aluminium-Zinc Alloy

V.D. Obasa [1*], M.O. Udo[2], C.O. Onegbedan[3], A.O. Ajayi[4], E.O. Addah[1], A.A. Yussouff [1]

[1] Department of Industrial and Systems Engineering, Lagos State University, Epe, Nigeria
[2] Department of Mechanical Engineering, Covenant University, Ota, Nigeria
[3]Department of Polymer and Textile Engineering, Federal University of Technology Owerri, Nigeria,
[4]Department of Computer Engineering, Lagos University of Technology, Ikorodu, Lagos, Nigeria.

ABSTRACT: This paper investigated the effects of pouring heights on macro-segregation, electrical and thermal conductivity of an Aluminium–Zinc alloy. Al 5wt.% Zn was cast at pouring heights ranging from 100 to 500 mm. Analytical techniques like optical scanning electron and energy dispersive spectrometry were used to assess the extent of segregation. The electrical and thermal conductivities were estimated, utilising the Wiedemann-Franz Law. The thermal profile of the as-cast Al-5wt.% Zn revealed variations in solidus and liquidus reaction temperatures relative to position, attributed to local chemical composition variation and cooling rate. Notably, at a pouring height of 400 mm, the temperature field in the melt was more uniform, leading to enhanced melt flow motion and transformation of large primary α-Al grains into finer spherical grains, resulting in a more homogeneous microstructure. As a result, the Al-5wt.% Zn sample obtained at a pouring height of 400 mm exhibited the highest electrical and thermal conductivities (37 IACS and 133 W/mK), aligning well with established standards (33.8% IACS and 131 W/mK). Significantly, the magnitude of macro-segregation recorded at various pouring heights even at low concentrations of solute (5wt.% Zn) signifies that macro-segregation strongly depends on the process parameter (i.e., pouring height) and not just the solute concentration.

KEYWORDS: Aluminum-Zinc Alloy, Pouring Height, Macro-segregation, Microstructural Analysis, Thermal Conductivity, Electrical Conductivity

[Received Jul. 2, 2024; Revised Sep 13, 2024; Accepted Oct 24, 2024] Print ISSN: 0189-9546 | Online ISSN: 2437-2110

I. INTRODUCTION

Solidification of molten metal during casting is a thermodynamic process motivated by several factors (Guan *et al.,* 2022) influencing its flow pattern and eventually the composition distribution (Benmaziane *et al.*, 2021). The variation in composition that occurs at the macroscopic level is termed macro-segregation. This phenomenon results from the movement or merging of localized micro-segregation. Micro-segregation is premised upon the fact that solutes are jettisoned by the solidifying front into the interdendritic slurry, making the region highly saturated with solute. This variation in concentration can be balanced by a subsequent hot working or annealing of the cast products, as it occurs over a short distance (10 - 100 μm) where diffusion can bring about a redistribution of the solute atoms (Obiekea *et al.*, 2018). However, macro-segregation is not easy to eliminate because it usually occurs over a long distance (1cm - 1m) where diffusion becomes ineffective (Muhrat *et al.*, 2018; Ghosh *et al*, 2001). Causes of macro-segregation can be a result of several factors such as density differences, solidification shrinkage, solute redistribution, and fluid flow. This is capable of weakening the mechanical properties of the cast structure and may compromise the structural integrity of the material leading to inconsistent performance. Since the composition of the alloy can vary across different regions, the performance of the material can become unpredictable.

Macro-segregation cannot be remedied once it occurs but, can only be prevented from happening by deploying the following mitigation strategies during the processing of the alloy; proper alloy design, stirring, controlled cooling, and ensuing directional solidification.

One of the important features exhibited during solidification is the change in phase from liquid to solid state along the solidification front. This leads to the release of latent thermal energy that is transferred through both phases. As-cast structures often exhibit macro-segregation of impurity elements, leading to non-uniform grain structures, with some areas having fine grains and others coarse grains (Fernando *et al.*, 2020). Coarse grain boundaries are often weaker and are potential paths for crack propagation, and localized corrosion sites (Cameron *et al.*, 2018; Ali *et al.*, 2021).

Macro-segregation can also induce variable resistivity due to heat flow discontinuity impacting the overall electrical performance of the cast. High resistivity regions can cause

*Corresponding author: victoria.obasa@lasu.edu.ng
doi: http://dx.doi.org/10.4314/njtd.v22i1.2710

increased energy losses, reduced efficiency in electrical systems and electromagnetic Interference (EMI) (Chouhan *et al.*, 2022). Also, non-uniform thermal conductivity can result in the development of thermal gradients within the material, affecting its thermal management performance. This can be particularly critical in applications requiring precise thermal control, such as in heat exchangers and engine components (Munekazu *et al*., 2019).

The effects of macro-segregation on electrical and thermal conductivity cannot be undermined because it leads to increased resistivity, inhomogeneous current distribution, reduced thermal conductivity and localized thermal gradients. This significantly poses processing challenges and impacts material performance. Controlling or mitigating macro-segregation is, therefore, germane in high-performance materials and components (Zhang *et al.*, 2023).

Thermal analysis has the potential to predict the effects of chemical changes such as composition variation on the resultant thermal curves and microstructural/mechanical properties of alloys (Marchwica *et al.*, 2012). However, precise prediction of thermal conductivity is quite difficult. Hence, recourse to the use of physical property that is uniquely connected to thermal conductivity. One of such property is electrical conductivity which roughly tracks thermal conductivity as captured by the Wiedemann-Franz law for metals. This is consequent to the fact that freely moving valence electrons transfer electric current and heat energy to their next neighbours (Clemens *et al.*, 2000). The interrelation between thermal and electrical conductivity stems from the shared role of free electrons in these processes. The Wiedemann-Franz law provides a valuable framework for understanding and predicting the behaviour of materials, particularly metals in terms of their conductive properties (Wei *et al.*, 2017; Devanathan, 2021). This law states that the thermal and electrical conductivity ratio is the same for all metals at a given temperature.

The Wiedemann-Franz law as a predictive tool is useful for predicting the thermal conductivity of a metal when its electrical conductivity is known. The temperature dependence of both conductivity properties is further established by this law. Notably, for pure metals at low temperatures, the law holds well, but there could be deviations at higher temperatures due to electron-phonon scattering.

Studies have also shown that the thermal conductivity of alloys and composites is a function of their volume fraction, concentration, distribution and conductivity of elemental components of the alloy (Ordonez-Miranda *et al.*, 2012). Usually, the presence of discontinuity owing to non-uniformity in the chemical composition of the alloy coupled with varied intermetallic phases brings about impediments in the flow of electrical or thermal energy within the alloy (Volklein *et al.*, 2009). This has been theoretically predicted and experimentally proven to majorly affect alloy conductivity (Obiekea *et al*, 2018). Therefore, this study examines the consequences of pouring heights on the propagation of macro-segregation in cast matrix and their eventual effects on the electrical and thermal properties of the Al_3Zn alloy.

II. METHODOLOGY

The base raw material used (1000 series aluminium, see Table 1) was obtained from Qualitech, Ojokoro, Lagos, Nigeria, while Zinc was sourced locally at Ojuire market in Ikorodu, Lagos Nigeria. An electronic analytical balance with 0.01g precision 13 units conversion, counting function, LCD and 5000 g capacity equipment was used to scale the raw materials into proportions suitable for charging into a steel pot. A *crucible* furnace was used for this melting operation consequent on the low melting point of zinc and aluminium. This was done in batches as stated in Table 1 to attain the desired concentration of the alloying element. Aluminium ($T_{m.p}$ = 660ºC) was charged first into the furnace before zinc ($T_{m.p}$ = 420ºC). When metals in the melting pot became molten, they were stirred together continuously until a uniform alloying was attained.

Moulds with cylindrical cavities of 30 mm by 300 mm were prepared from green sand, bentonite and silica flour, which improved the surface finish by providing resistance to metal penetration. The A flange is crewed to the desired pouring height and the molten metal is poured out at this referenced height into the mould.

The temperature profile of the liquid metal and solidifying cast were taken using a K-Type digital thermocouple with error limits of +/- 1.1ºC**.** The recorded temperatures at specified times were used to generate experimental cooling curves. The experimental flow chart in Figure 2 is a summary of the methodological approach adopted in this research work.

Table 1: Elemental Composition of 1000 Series of Aluminium alloy

Elements	Cu	Fe	Mg	Mn	Si	Ti	Zn	Al
% Composition	0.03	0.15	0.02	0.02	0.2	0.02	0.06	99.55

Table 2: Elemental Composition of Aluminium Zinc Alloy

Elements	% Al	% Zn	% Si	% Mg	% Fe
%Composition	93.000	5.000	1.301	0.048	0.451

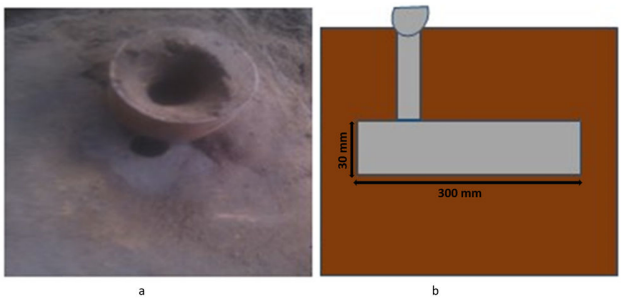

Figure 1: The experimental setup of the (a) mould block and (b) internal mould configuration.

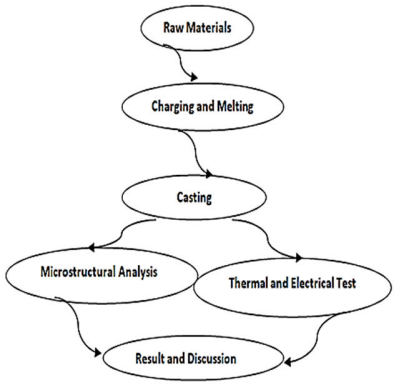

Figure 2: The schematic representation of the methodology.

A. Electrical Conductivity Test

The electrical conductivity test began with carrying out a resistivity test for the cast samples using a BEKO power AB TYPE – Rm 0606, 110/240 V AC. Firstly, a circuit using a power supply, variable resistor, wires, crocodile clips, an ammeter and the Al_3Zn rod to be tested.

The average diameter of the Al_3Zn rod was obtained using a micrometre screw gauge and with this, the area of the rod was calculated. Using a meter ruler, the length of the rod was also determined. At varied lengths on the rod, current and potential difference measurements were taken and these were then used to compute the resistance, resistivity, electrical and thermal conductivity of the rod with reference to equations 1 to 4. For each setup, a minimum of ten successive readings were recorded for the parameter being estimated.

$$R = \frac{V}{I} \quad (1)$$

$$\rho = \frac{RA}{l} \quad (2)$$

$$\sigma = \frac{1}{\rho} \quad (3)$$

$$k = \sigma LT \quad (4)$$

Where σ is the electrical conductivity in $\Omega^{-1}m^{-1}$, ρ is the resistivity in Ω, k is the thermal conductivity in W\mK, T is the absolute temperature in K, and L is the Lorenz number, which is equal to 2.45 10^{-8} WΩ/K^2.

B. Sample Preparation for Microstructural Examination

Microstructural study was carried out using optical analysis, Scanning Electron Microscopic (SEM), and Energy Dispersive Spectroscopic (EDS) examinations. The samples for microstructural examination were sectioned at the ends and middle sections of the coupons following the ASTM E3 standard procedure. This was further subjected to polishing using varied sizes of emery paper from 120, 240, 320, 600 to 1200 at 200 rmp until the desired smoothness was achieved. The etching process was carried out at room temperature according to ASTM E407 – Standard Practice for Microetching Metals and Alloys. Upon polishing the surfaces of the samples were swabbed with Weck's Reagent (100 mL water, 4 g $KMnO_4$, and 1 g NaOH) for about 15 seconds, washed and dried to prevent scratches on the finished surface. This process was immediately followed up by subjecting the specimens to microscopic examination. The captured images were at a magnification of 200 µm. The same set of samples was further subjected to EDS and SEM analysis on the Phenon proX SEM machine, model number 80007334 and part number MVE0224651193. It operated with an electron intensity beam of 15 kV while the samples were mounted on a conductive carbon imprint left by the adhesive. Samples were placed on a circular holder and coated for 5 min to enable it to conduct electricity.

III. RESULTS AND DISCUSSION

A. Cooling Profile of Al-Zn Alloy

The cooling profile in Figure 2 reveals that solidification begins at a liquidus temperature of 720°C at a cooling rate of 0.95°C/s. As solidification proceeded, there was a significant drop in the temperature of the cast from 720°C to 640°C as solute atoms were rejected at the solid-liquid interface into the slurry. Beyond this stage, the temperature was maintained at 640°C from 80 to 200 s and later decreased progressively as the time increased for all the samples under consideration. It was worth noting that at a stage when the temperature became equitably constant, it is attributable to the dissipation of latent heat of solidification (h_l) (Liu *et al*., 2014). This liberated heat energy markedly affects the rate and mode of crystal growth. The general fall in temperature to give room for freezing causes a lowering of the solubility of the alloying elements in the melt. The solubility of the alloying elements is further affected as a result of the changed composition of the alloy grossly affecting the final structure of the solidified melt.

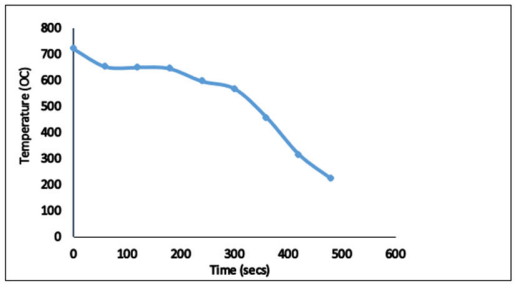

Fig. 2: Cooling curve for Al 5wt.% Zn alloy

B. Effects of Varied Pouring Heights on Cast Microstructure

Zinc has about 0.85% solubility in aluminium hence, Al 5wt%Zn, which is the lowest concentration under consideration was used. Regardless of the small amount of zinc (5wt.%) that was used, cast samples still exhibited significant segregation. In Figure 3, it can be observed that the segregation of solute atoms was more prominent around the centre of the billet while at the periphery of the cast, consequent on the rapid cooling at the mould wall and lowered cooling rate at the centre region of the cast (Rominiyi *et al.*, 2018). The rapid cooling at the mould wall interphase does not give room for the diffusion of solute, hence explaining the absence of segregation at this region. Further away, as the solidification rate is lowered there is solute rejection from the solidifying melt into the solidifying front at the centre of the billet accounting for the high level of segregation.

At the pouring height of 400 mm, the sample showed an improved distribution of solute elements compared to other pouring heights. This improved structure is relatable to a more uniform fluid flow engendered at this pouring height as predicted by Li *et al.*, (2023). Hence, it can be inferred that samples at this pouring range are better off and less segregated. The above phenomenon termed heterogeneous nucleation has been exhaustively discussed (Riahi, 2002; Galenko *et al.*, 2017). This heterogeneous nucleation occurs as a result of convective effects, which initiate a favoured site for nucleation.

Figures 4 to 8 show the optical and scanning electron microstructures of cast samples while Table 3 depicts the variation in elemental compositions of the aluminium zinc alloy. The following microstructural phases were identified: Al-matrix (white), Al5FeSi (brown), $AlSiO_2$ (ash), and different the presence of multicomponent phases containing Mg_2Zn11, $A_{l2}CuMg$ (different dark shades) (Malakho *et al.*, 2010; Mrówka-Nowotnik *et al*, 2007). These are known to be responsible for the loss of permeability in the mushy zone that occurs during alloy solidification (Adam, 2005; Zhang *et al.*, 2015).

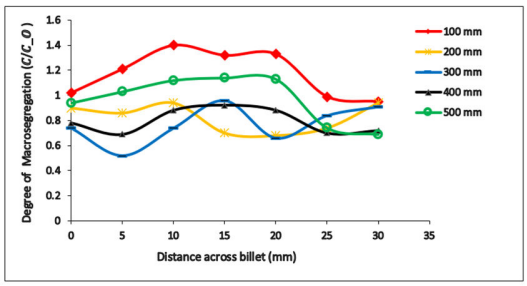

Figure 3: Graph showing the effect of pouring height on segregation in Al 5wt.% Zn

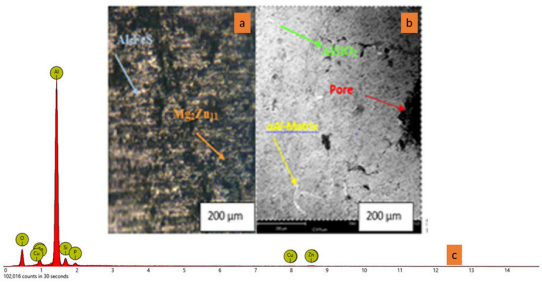

Figure 4: Al 5wt.% Zn at 100 mm (a) Optical Micrograph (b) SEM Micrograph (c) EDS spectrum

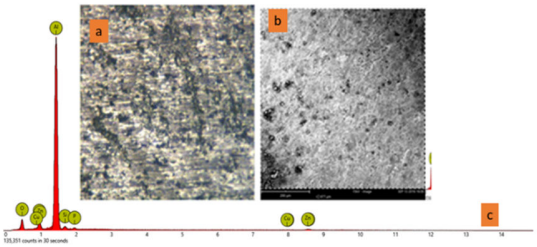

Figure 5: Al 5wt.% Zn at 200 mm (a) Optical Micrograph (b) SEM Micrograph (c) EDS spectrum

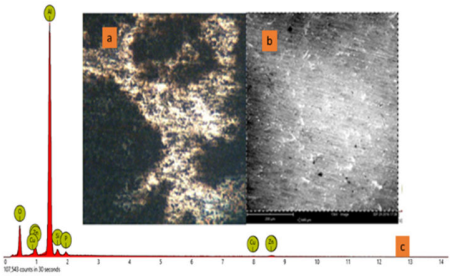

Figure 6: Al 5wt.% Zn at 300 mm (a) Optical Micrograph (b) SEM Micrograph (c) EDS spectrum

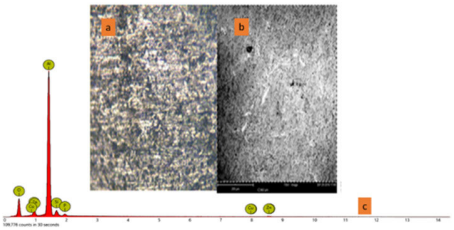

Figure 7: Al 5wt.% Zn at 400 mm (a) Optical Micrograph (b) SEM Micrograph (c) EDS spectrum

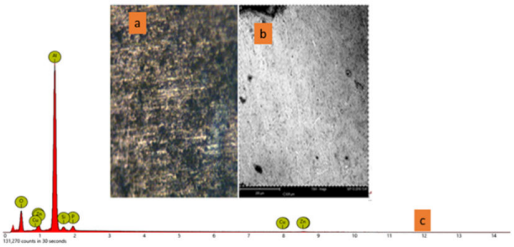

Figure 8: Al 5wt.% Zn at 500 mm (a) Optical Micrograph (b) SEM Micrograph (c) EDS spectrum

Table 3: Variable elemental composition of the Al-Zn cast

Element	100 mm	200 mm	300 mm	400 mm	500 mm
Al (%)	70.8	62.5	71.5	65.2	59.4
O (%)	17.5	25.1	20.1	24.9	30.7
Si (%)	2.4	4.7	2.7	3.1	2.4
P (%)	1.6	2.1	1.5	1.4	1.4
Zn (%)	6.0	4.3	3.7	4.4	4.8
Cu (%)	1.6	1.3	0.6	1.0	1.3

C. Electrical and Thermal Properties of Al-Zn Alloy

Figures 9 and 10 display an excellent agreement with the pattern of macro-segregation analysed in Figure 3. The Al-Zn cast sample fed at 400 mm pouring height gave the highest conductivity values of 37 IACS and 133 W/mK. This confirms that macro-segregation significantly influences the conductivity of cast samples as established in the preceding section where cast produced at 400 mm exhibited less inhomogeneity/segregation in its composition. The findings of the study compared favourably with the findings reported by Payandeh *et al,* (2016). It was reported that macro-segregation brings about discontinuities to consistent inflow of thermal and electrical properties from one point to the other in cast products.

A decrease in the magnitude of inhomogeneity engenders a more lucid structure, which enhances uniform heat flow (Ikumapayi *et al.,* 2018; Ikumapayi *et al.,* 2019). When there is a near-homogenous structure, the thermal barriers are reduced, leading to enhancement in the thermal and electrical characteristics of the casting (Mulaba-Kapinga *et al.,* 2020; Lokesh *et al.,* 2020).

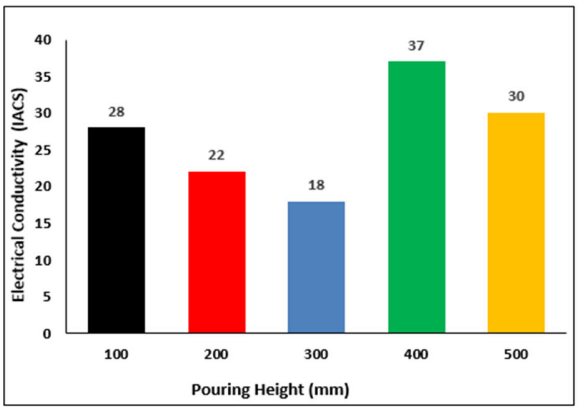

Figure 9: Electrical conductivity of Al 5wt.% Zn Alloy with pouring height

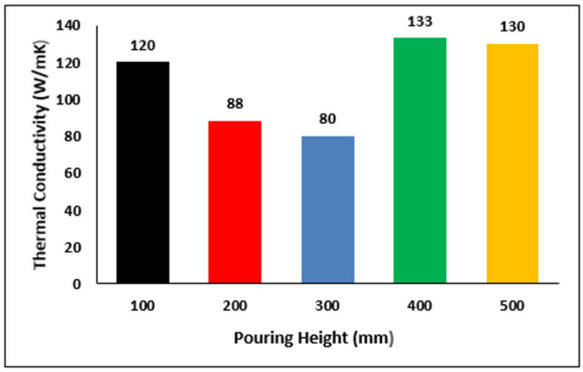

Figure 10: Thermal Conductivity of Al 5wt.% Zn Alloy with pouring height

IV. CONCLUSION

The study on the pouring height effect on macro-segregation of aluminium-zinc alloy has been carried out relative to its thermal and electrical behaviours. Summarily, the current study contributes to the existing knowledge by establishing the fact that the control of molten metal pouring height can significantly reduce macro-segregation during the solidification of molten aluminium binary alloy with concomitant improvement in in-service properties. This in effect culminates into an upgrade in thermal and electrical characteristics of the cast product useful in electrical and electronics industries.

AUTHOR CONTRIBUTIONS

Obasa, V.D. - Conceptualization; Methodology; Experimentation Investigation; Writing - original draft**; Udo M.O.-** Data curation; Formal analysis; Investigation; **Onegbedan C.O.** – Methodology & review **Ajayi A.O.** Conceptualization; Methodology; **Addah E.O**. - review & editing, **Yussouff A.A.** - review & editing.

REFERENCES

Ali, N.; L. Zhang; H. Zhou; A. Zhao; C. Zhang; K. Fu, and J. Cheng. (2021). Investigation on Internal Crack Defects in Medium Carbon Steel by Soft Reduction. Materials Research. 24: 10.1590/1980-5373-MR-2021-0055.

Benmaziane, S.; O. Ben lenda; L. Zerrouk and E. Saad. (2021). Numerical Modelling of Copper Macro-segregation in the Binary Alloy Al-4Cu E3S Web of Conferences 229, 01015 (2021). ICCSRE'2020.

Cameron, B.; S. Shi; E. Mark; N. Orchowski; N. Matthews, and M. Brandt. (2018). Influence of Macro-segregation on Solidification Cracking in Laser Clad Ultra-High Strength Steels. Surface and Coatings Technology. 340. 10.1016/j.surfcoat.2018.02.052.

Chouhan, A.; M. Hesselmann; A. Toenje; L. Mädler and N. Ellendt. (2022). Numerical Modelling of In-Situ Alloying of Al and Cu Using the Laser Powder Bed Fusion Process: A Study on the Effect of Energy Density and Remelting on Deposited Track Homogeneity, Additive Manufacturing. 59:

Clemens, J.M. (2000). How Thermal conductivity relates to electrical conductivity. Technical Data, Test & Measurement 6 (2):1-6.

Devanathan, V. (2021). The Wiedemann-Franz Law for Electrical and Thermal Conduction in Metals. 4: 1-26.

Fernando P.Q.; J.L. Wysllan; G.P. Késsia; C. S. Roberto; A.S.B. Luis, and A. F. Ferreiraa. (2020). An Experimental Investigation of Continuous Casting Process: Effect of Pouring Temperatures on the Macro-segregation and Macrostructure in Steel Slab. Materials Research. 23 (4): e20200023.

Galenko, P.K.; D.A. Danilov; K. Reuther; D.V. Alexandrov; M. Rettenmayr and D.M. Herlach. (2017). Effect of convective flow on stable dendritic growth in rapid solidification of a binary alloy. Journal of Crystal Growth. 457 (1): 349-355.

Ghosh, A. (2001). Segregation in Cast Products. Sadhana, 26: 5–24.

Guan, J.; Z.P. Pu; S.C. Zhao and D.R. Liu. (2022). Three-Dimensional Modeling of Segregation Behavior during

Solidification of a Sn-6 wt.% Pb Alloy. Materials (Basel). 15 (4):1298.

Li, Y; W. Chen and Y. Sun. (2023). Analysis of macro-segregation during slab continuous casting using a 3D-longitudinal 2D hybrid model. Ironmaking and Steelmaking. 50 (7): 794-808. doi:10.1080/03019233.2023.2190255

Liu, Y.; M. Liu; L. Luo; J. Wang, and C. Liu (2014). The solidification behaviour of AA2618 aluminium alloy and the influence of cooling rate. Material. 7: 7875-7890.

Malakhov, V.; P. Dmitri; G. Damon and M Mark. (2010). On the formation of intermetallics in rapidly solidifying Al–Fe–Si alloys. Calphad. 34 (2): 159-166.

Marchwica, P. (2012). Microstructural and Thermal Analysis of Aluminium-Silicon and Magnesium-Aluminium Alloys Subjected to High Cooling Rates, Electronic Thesis and Dissertations, University of Windsor.

Mrówka-Nowotnik G.; J. Sieniawski, and M. Wierzbiñska. (2007). Intermetallic-phase-particles-6082
Muhrat, A. (2022). Ultrasound-Assisted Low-Temperature Brazing of Titanium/Titanium Joints Using Aluminium Filler Alloys. Cross Ref.

Munekazu, O.; Y. Masayoshi and M. Kiyotaka. (2019). Importance of Microstructural Evolution on Prediction Accuracy of Micro segregation in Al-Cu and Fe-Mn Alloys, International Journal of Heat and Mass Transfer, 132: 1004-1017.

Obiekea, V.D.; I.O. Sekunowo, M.G. Sobamowo, and S.O. Adeosun. (2018). Study of macro-segregation effects on thermal and electrical characteristics of aluminium-copper alloy. ACTA TECHNICA CORVINIENSIS – Bulletin of Engineering. 3:35-38.

Obiekea, V.D.; I.O. Sekunowo; M.G. Sobamowo and S.O. Adeosun. (2018). Effects of Casting Speed and Runner Angle on Macro-segregation of Aluminium-Copper Alloy, JCAMECH. 49(2): 373-379.

Ordonez-Miranda, J. and J.J. Alvarado-Gil. (2012). Thermal Conductivity of Nanocomposites with High Volume Fractions of Particles. Composites Science and Technology. 72 (7): 853-857.

Riahi, D.N. (2002). Effects of Rotation on Convection in a Porous Layer During Alloy SolidificationTransport Phenomena in Porous Media II, book.

Rominiyi, A.L; D. Isadare; M. Adeoye; K. Akinluwade and A. Adetunji. (2015). Effect of As-Cast Cooling on the Microstructure and Mechanical Properties of Age-Hardened 7000 Series Aluminium Alloy. International Journal of Materials Engineering, 5 (1): 5-9

Volklein, F.; H. Reith; T.W. Cornelius and M. Rauber (2009). The experimental investigation of thermal conductivity and the Wiedemann–Franz law for single metallic nanowires. IOP Science, Nanotechnology. 20 (32): 1-8.

Wei, C.; N. Antolin; O.D. Restrepo; W. Windl and J. Zhao. (2017). A General Model for Thermal and Electrical Conductivity of Binary Metallic Systems, Acta Materialia. 126 (7):272-279

Zhang, Y.; X. Liu; Q. Zhu; Y. Zuo; R. Wang and H. Jiang. (2024). Understanding of Macro-Segregation in Direct-Chill Cast 2024 Alloy with Intensive Melt Shearing Based on the Evolution of Microstructure and Temperature Field, Journal of Materials Research and Technology. 27: 7766-7777.